Conformational Changes in Diethylene Glycol Dimethyl Ether and Poly(ethylene oxide) Induced by Lithium Ion Complexation

Roger Frech* and Weiwei Huang

Department of Chemistry and Biochemistry, University of Oklahoma, Norman, Oklahoma 73019

Received June 2, 1994; Revised Manuscript Received September 23, 1994®

ABSTRACT: Conformational changes in diethylene glycol dimethyl ether (diglyme) and high molecular weight poly(ethylene oxide) induced by complexation with lithium trifluoromethanesulfonate ($LiCF_3SO_3$) have been investigated using Raman scattering and infrared transmission spectroscopy. In both the diglyme and polymer complex new bands were observed in spectral regions involving a significant amount of CH_2 bending motion. These bands are attributed to a conformation which is not energetically favored in the pure polymer or oligomer but which is stabilized through interactions of the cation with the polyether oxygen atoms. The structure of the new conformer is discussed.

1. Introduction

There are a number of factors which play a role in the mechanism of ionic transport in ionically-conducting polymers consisting of poly(ethylene oxide) (PEO) complexed with metal salts. One of the most important factors is the interaction of the cation with the polymer.[1−4] The cations are coordinated by the ether oxygen atoms of the polymer backbone which leads to the solubilization of the salt and the formation of a polymer−salt complex. This interaction may be expected to affect the local structure of the polymer backbone. The local structure can be conveniently described by the relative internal rotations of the consecutive single bonds comprising the polymer backbone, i.e., by the conformation. Conventionally, T refers to a trans arrangement, G is a gauche arrangement, and G′ is a gauche arrangement in the opposite direction with respect to G. In a description of the conformation, it is important to define the sequence of bonds being characterized. For example, the conformation of high molecular weight PEO is given as $(T_2G)_4$,[5] referring to the bond sequence C−O−C−C. In this study, comparisons will be made between salt complexes of high molecular weight PEO and corresponding salt complexes of glymes with the general formula $CH_3(OCH_2CH_2)_nOCH_3$. In the glymes it is customary to describe the conformation of the bond sequence O−C−C−O. Consequently the conformations of the high molecular weight PEO complexes will also be referred to this sequence.

X-ray diffraction studies of polymer conformation in crystalline polymer−salt complexes show that the conformation of pure, high molecular weight PEO is altered upon complexation with metal salts.[6−9] Vibrational spectroscopy has also been used to examine such conformational changes.[10] A number of studies illustrating the conformational change in high molecular weight PEO induced by complexation are summarized in Table 1.

Conformations of both liquid and solid glymes where n = 1, 2, 3, and 6 have been extensively studied using vibrational spectroscopic methods.[11−13] Liquid glymes often exist in several conformations, whereas solid glymes have the same helical conformation found in solid high molecular weight PEO.[14] The conformation of glymes can also be modified by complexation with metal salts, and studies of these systems provide additional insight into questions of local structure and conformation. A TGT−TG′T−TGT conformation was observed in the central part of the chain in a heptaethylene glycol complex with $Sr(SCN)_2$.[15]

Table 1. Conformations of Crystalline PEO and PEO−Salt Complexes

compound	conformation: C−O−C−C	conformation: O−C−C−O	ref
PEO	$(T_2G)_4$	$(TGT)_4$	5
$(PEO)_3NaSCN$	$(T_2GT_2GT_2G')_2$	$(TGT)_2(TG'T)$	6
(PEO)(NaSCN)	$TG_2TG'_2$	(GGT)(G′G′T)	6
$(PEO)_3NaI$	$(T_2GT_2GT_2G')_2$	$(TGT)_2(TG'T)$	7
$(PEO)_4HgCl_2$	T_5GT_5G'	(TTT)(TGT)(TTT)(TG′T)	8
$(PEO)(HgCl_2)$	$TG_2TG'_2$	(GGT)(G′G′T)	9
$(PEO)_{4.5}NaX$ (X = Br, I, SCN, BF_4)	T_2GT_2G'	(TGT)(TG′T)	10

We previously reported a Raman spectroscopic study of the CH_2 rocking region of several glymes complexed with metal salts and suggested that the interaction of the cation with the polyether oxygens occurs, with the glyme adopting a conformation which is energetically unfavorable in the pure liquid.[16] A study of the chain length dependence of the new conformer bands showed that the conformation adopted by the diglyme complex was slightly different than that of the monoglyme, triglyme, and tetraglyme complexes. A dependence of the new conformation band frequency on the nature of the cation was also observed.

In this paper we will compare complexes of lithium trifluoromethanesulfonate ("triflate"; $LiCF_3SO_3$) prepared with the n = 2 glyme and with high molecular weight PEO. Both complexes are prepared at a 5:1 ether oxygen to cation ratio. This study will consider a number of bands in several spectral regions which are sensitive to conformational changes in the polymer backbone.

2. Experimental Section

The diglyme (Aldrich; anhydrous, 99+%) was used without further purification. Lithium triflate (Aldrich; 97%) was dried at 140 °C under vacuum for 24 h before use. The diglyme complexes were prepared under a dry nitrogen atmosphere in a glovebox. No solvent was used in the complexation process.

The PEO−lithium triflate complex was prepared in a glovebox filled with dry nitrogen by separately dissolving the required amounts of the polymer and the vacuum-dried

® Abstract published in *Advance ACS Abstracts,* January 15, 1995.

0024-9297/95/2228-1246$09.00/0

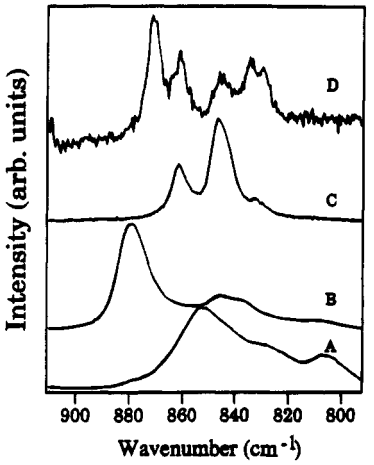

Figure 1. Raman scattering spectra in the CH_2 rocking spectral region: (A) pure diglyme; (B) 5:1 diglyme–LiTf complex; (C) pure PEO; (D) 5:1 PEO–LiTf complex.

lithium triflate salt in anhydrous acetonitrile and then mixing the two solutions. After continuous stirring for 24 h at room temperature, the solution was allowed to stand at room temperature for a further 24 h to facilitate degassing. The gelatinous polymer solution was then cast on a Teflon support. Films to be used for infrared spectral data collection were cast on a barium fluoride window. Subsequent solvent evaporation led to bubble-free and pinhole-free uniform films of 20–30 μm thickness. The films were dried overnight in vacuum at 120 °C. Pure PEO films were prepared by the same method without mixing the salt.

Parallel polarized Raman spectra of samples contained in a capillary were recorded at room temperature using a standard 90° scattering geometry. A 0.85 m Czerney–Tuner double monochromator equipped with a thermoelectrically cooled RCA (31034) photomultiplier tube was used for data collection. The light source was the 488.0 nm line excited at 400 mW from a Spectra Physics argon ion laser. Infrared spectra were collected on a Bio-Rad FTS 40 Fourier transform infrared spectrometer at 1 cm^{-1} spectral resolution. Barium fluoride windows were used in a variety of standard liquid cells for the glyme and glyme-complex spectra. In the low-frequency region the absorption due to the windows was subtracted from the transmission spectra.

3. Results

This study focuses on those vibrational modes which involve a significant amount of CH_2 bending motion. As will be shown later, to a reasonably good approximation these modes in each ethylene oxide subunit of the diglyme molecule appear to be vibrationally decoupled from the adjacent subunit. Therefore, in discussing the vibrational spectral data of the diglyme and diglyme–salt complexes, it is both permissible and useful to use vibrational assignments for conformers of the well-studied monoglyme compound.

Figure 1 compares Raman scattering spectra of pure and complexed diglyme with the corresponding spectra of high molecular weight PEO. This is a spectral region in which the bands are a mixture of CH_2 rocking and CO stretching motions.[13] To facilitate discussion here, these modes will be referred to simply as CH_2 rocking vibrations. Curves A and B of Figure 1 are spectra of the pure diglyme and the corresponding 5:1 (ether oxygen–metal cation) complex. In curve A, the spectrum of the diglyme, the band at 853 cm^{-1} is assigned to the TGT conformer with some contribution from the TGG conformer, while the band at 822 cm^{-1} is assigned to the TTG conformer with some contribution from the TTT conformer.[11] The band at 808 cm^{-1} is attributed to the trans conformation of the OCH_2–CH_2O group.[13]

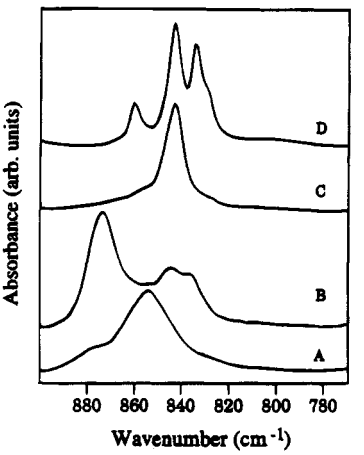

Figure 2. Infrared absorbance spectra in the CH_2 rocking spectral region: (A) pure diglyme; (B) 5:1 diglyme–LiTf complex; (C) pure PEO; (D) 5:1 PEO–LiTf complex.

The most striking change in this region upon complexation with lithium triflate is the growth of a new band at 879 cm^{-1} with increasing salt concentration, while the band at 853 cm^{-1} correspondingly decreases in intensity. There are also other, more subtle spectral changes which will be subsequently discussed. Since the bands in the pure oligomers originate in the vibrations of distinct conformers, we assign this new band in the complex to the CH_2 rocking vibration of an oligomer conformation which is not observed in the pure liquid but is adopted by the oligomer in order to coordinate the lithium ion upon formation of the complex.[16]

This general pattern is also seen in spectra of PEO (curve C) and the PEO complex (curve D), although there are some significant differences. Since the overall composition of the PEO–lithium triflate system is 5:1, it is clear from the phase diagram[17] that at room temperature this composition corresponds to a two-phase region consisting of pure PEO and a 3:1 compound of PEO–lithium triflate. The spectrum of the complex appears to be a superposition of the pure PEO spectrum and additional bands which can be attributed to the 3:1 compound. The increase in frequency of the band at 871 cm^{-1} relative to the pure polymer band at 861 cm^{-1} strongly suggests that there is a change in the local conformation of the polymer upon complexation which is similar to the change in the glyme upon complexation.

It is important to complement the Raman data with infrared absorption spectra in this region. Figure 2 compares the infrared spectra of diglyme, diglyme complex, PEO, and PEO complex in the same manner as in Figure 1. In the pure glyme (curve A) the relatively strong band at 855 cm^{-1} decreases in intensity and a new band at 874 cm^{-1} increases with increasing salt concentration. In order to interpret this behavior, it is helpful to examine Figure 3, which illustrates in greater detail the concentration dependence of the infrared bands of the diglyme complexes. The intensity of the very weak band at 874 cm^{-1} in the pure glyme increases with salt concentration, while the strong band at 855 cm^{-1} decreases in intensity. In the 20:1 complex (curve C), a weak shoulder at 844 cm^{-1} is seen on the low-frequency side of the 855 cm^{-1} band. In the 10:1 complex (curve D) the intensity of this shoulder continues to grow while another feature is noted at 836 cm^{-1}. Finally, in the 5:1 complex (curve E), there are the two bands at 845 and 836 cm^{-1}, previously observed as

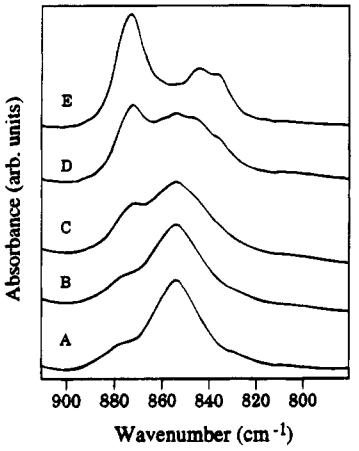

Figure 3. Salt concentration dependence of the Raman scattering spectra of the diglyme–LiTf complexes in the CH_2 rocking spectral region: (A) pure diglyme; (B) 80:1 complex; (C) 20:1 complex; (D) 10:1 complex; (E) 5:1 complex.

Table 2. Frequencies (cm^{-1}) of Diglyme, the 5:1 Diglyme–LiTf Complex, PEO, and the 5:1 PEO–LiTf Complex

assignment	diglyme	diglyme–LiTf	PEO	PEO–LiTf
CH_2 rock & CO stretch		879		871
(Raman-active modes)	853		861	861
		845	846	845
		836	832	834
	822			829
	808			
CH_2 rock & CO stretch	874	874	857	860
(infrared-active modes)	855	845	843	843
		836		834
			828	830
CO stretch & CH_2 rock	986	986		
(infrared-active modes)	983	983		
				969
	967		963	965
				957
	939	947	949	952
	932	931	934	
CH_2 wag (infrared-active	1370	1376		1367
modes)			1360	1360
	1354	1352		1352
			1343	1343
				1340
CH_2 scissors (infrared-	1489	1476	1475	1476
active modes)	1471		1467	1470
		1460		1461
	1453		1455	1454

shoulders, and the strong feature at 874 cm^{-1}, all of which are assigned to the new conformer. Returning to Figure 2, the spectral behavior of the PEO complex is now seen to be quite similar to that of the glyme complex. In the spectrum of pure PEO, a strong band is observed at 843 cm^{-1} with very weak features at 857 and 828 cm^{-1}. With increasing lithium triflate concentration, two new bands grow in at 860 and 834 cm^{-1}, with a weaker feature also noted at about 830 cm^{-1}. These observations further argue that the dominant conformation of the diglyme complex is quite similar to the local conformation of the crystalline compound in the PEO complex. The frequency data of Figures 1 and 2 are summarized in Table 2.

A comparison of the infrared and Raman spectra of both PEO and the 5:1 PEO–lithium triflate complex is shown in Figure 4. The frequency of the intense band assigned to the 3:1 compound in the PEO complex is observed at 871 cm^{-1} in the Raman spectrum (curve D) and 860 cm^{-1} in the infrared spectrum (curve B). These

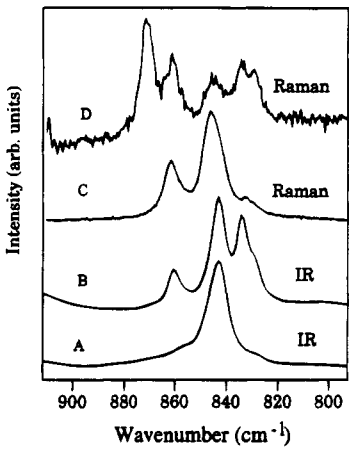

Figure 4. Comparison of the infrared and Raman spectra of PEO and the 5:1 PEO–LiTf complex in the CH_2 rocking spectral region: (A) IR spectrum of pure PEO; (B) IR spectrum of a 5:1 PEO–LiTf complex; (C) Raman spectrum of pure PEO; (D) Raman spectrum of a 5:1 PEO–LiTf complex.

observations are consistent with the crystal structure of this compound recently published by Lightfoot et al.,[18] who characterized the structure with the monoclinic space group $P2_1/a$ (C_{2h}^5). The isomorphous unit cell group contains a center of symmetry, with the consequence that vibrational modes which are active in a Raman scattering experiment are necessarily inactive in an infrared absorption measurement, and vice versa. The behavior of the Raman and infrared spectral data of pure PEO is similar to that of the PEO complex, with dominant Raman-active components at 861 and 846 cm^{-1} (curve C) and corresponding infrared-active components at 857 and 843 cm^{-1} (curve A). This is expected, since the space group of crystalline PEO is also $P2_1/a$ (C_{2h}^5).[19]

Although this spectral region has been previously assigned to the CH_2 rocking vibration of the oligomer mixed with some CO stretching motion, it is important to confirm that the intense Raman-active band observed at 879 cm^{-1} in the salt complex is indeed due primarily to the CH_2 rocking vibration of the oligomer with very little contribution, if any, from the oxygen-cation breathing mode.[10] Therefore, Raman scattering spectra of the diglyme and the 20:1 diglyme–lithium triflate complex are compared with spectra of the deuterated (d14) diglyme and the deuterated (d14) diglyme complex in Figure 5. At this concentration, contributions from both the uncoordinated diglyme and the diglyme coordinated by a lithium ion can be easily seen. The spectral pattern in the CH_2 rocking region is faithfully reproduced at lower frequencies in the deuterium-substituted complex. The band due to uncoordinated diglyme, observed at 853 cm^{-1} in the diglyme–salt complex, is shifted to 720 cm^{-1} in the deuterated diglyme–salt complex with a frequency shift ratio (ν_D/ν_H) of 0.844. The corresponding bands originating in the coordinated diglyme are observed at 879 and 740 cm^{-1}, respectively, with a ν_D/ν_H ratio of 0.842. The isotopic frequency shift data of both the pure glyme and the coordinated glyme establish that these modes contain not only a significant amount of CH_2 motion but very similar kinds of CH_2 motion.

The spectral region from 900 to 1000 cm^{-1} in PEO systems has also been assigned to CO stretching motion mixed with CH_2 rocking vibrations[13] and therefore reflects the local conformational changes occurring upon complexation in both diglyme and high molecular weight PEO. A comparison of spectral changes in these

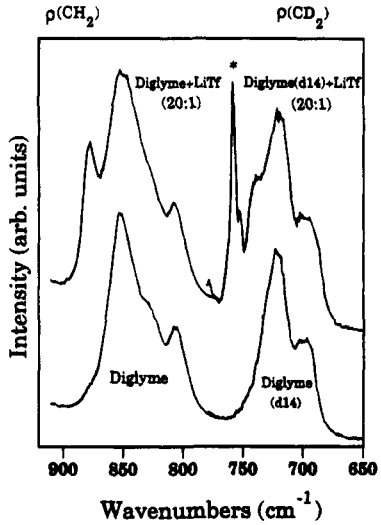

Figure 5. Raman scattering spectra of the diglyme, deuterated (d14) diglyme, and the corresponding 20:1 LiTf complexes in the CH_2 rocking region. The asterisk designates the CF_3 symmetric deformation mode of the triflate anion.

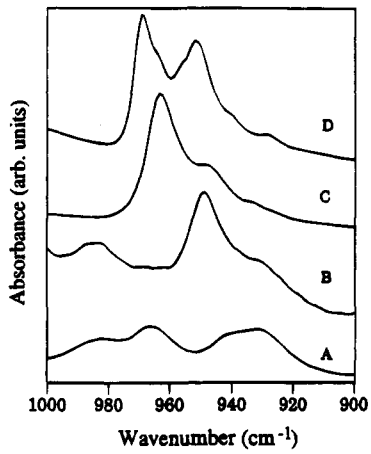

Figure 6. Infrared absorbance spectra in the 900–1000 cm^{-1} spectral region: (A) pure diglyme; (B) 5:1 diglyme–LiTf complex; (C) pure PEO; (D) 5:1 PEO–LiTf complex.

two systems upon complexation is shown in Figure 6. Here the band at 967 cm^{-1} in the diglyme (curve A) disappears, while a strong new band at 947 cm^{-1} appears in the complex (curve B). In addition, the intensity of a feature at 983 cm^{-1} in the diglyme appears to increase with increasing salt concentration in the complex. In the high molecular weight PEO–salt complex (curve D), new bands occur at 952 and 969 cm^{-1}. As before, the complex should be viewed as a superposition of two phases, with the dominant band at 963 cm^{-1} in pure PEO also seen in the complex as a shoulder on the new band at 969 cm^{-1}.

There are other vibrational modes which contain a significant amount of CH_2 motion and also appear to be sensitive to local conformation. Spectra from the CH_2 wagging region are shown in Figure 7, in the same display format as in Figures 2 and 6. In the diglyme (curve A) there is a small shift of the strong band at 1354 to 1352 cm^{-1} and a 6 cm^{-1} increase of the glyme band at 1370 cm^{-1} upon complexation (curve B). In pure PEO (curve C) the two strongest bands in this region, at 1343 and 1360 cm^{-1}, appear at 1340 and 1367 cm^{-1}, respectively, in the complex (curve D). In addition, a new band is seen at 1352 cm^{-1} in the complex which may correspond to the high-frequency shoulder of the 1343 cm^{-1} band in the pure PEO. Similar

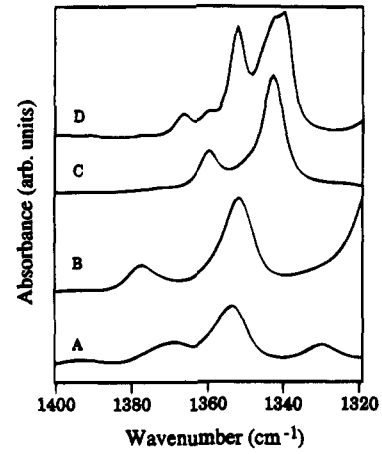

Figure 7. Infrared absorbance spectra in the CH_2 wagging spectral region: (A) pure diglyme; (B) 5:1 diglyme–LiTf complex; (C) pure PEO; (D) 5:1 PEO–LiTf complex.

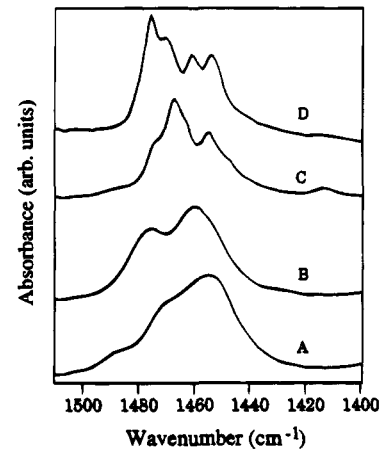

Figure 8. Infrared absorbance spectra in the CH_2 bending spectral region: (A) pure diglyme; (B) 5:1 diglyme–LiTf complex; (C) pure PEO; (D) 5:1 PEO–LiTf complex.

behavior is noted in the CH_2 in-plane bending or "scissors" region shown in Figure 8. The two bands at 1453 and 1489 cm^{-1} in the diglyme (curve A) become bands at 1460 and 1476 cm^{-1} in the complex (curve B). Similarly the two bands at 1455 and 1467 cm^{-1} in PEO (curve C) are shifted to 1461 and 1476 cm^{-1} in the complex (curve D). The frequency data of Figures 6–8 are also summarized in Table 2.

4. Discussion

The TGT–TGT conformation of the diglyme is described by the C_2 point group, with the consequence that the symmetry species of the CH_2 rocking vibrations are $\Gamma(\varrho,CH_2) = 2A + 2B$. Comparative spectroscopic studies of the $n = 1-4$ glymes suggest that the higher frequency modes in each ethylene oxide unit are relatively decoupled. Locally there is an effective C_2 axis bisecting the C–C bond of each ethylene oxide subunit, and the two CH_2 rocking modes of each subunit can be approximately described by the symmetry species $\Gamma(\varrho,CH_2) \approx A + B$. Since the vibrations of two ethylene oxide subunits are somewhat decoupled, results of calculations in the monoglyme system can be used to provide important insight into the diglyme system. Murcko and DiPaola have calculated ab initio vibrational frequencies as a function of conformation in 1,2-dimethoxyethane (monoglyme) at the 3-21G and 6-31G* levels.[20] In their calculation the frequency of the A-type symmetry spe-

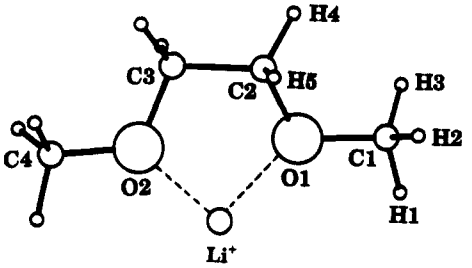

Figure 9. Optimized geometry of the monoglyme–Li^+ complex at the HF/6-31 G level.

Table 3. Optimized Geometries (Bond Lengths in Å, Angles in Degrees) and Total Energies (Hartrees) of PEO Monoglyme and PEO Monoglyme Complexed with Lithium Triflate (Basis Set HF/6-31G)

coordinate	monoglyme	monoglyme complex
$r(C_1-O_1)$	1.423	1.451
$r(O_1-C_2)$	1.425	1.450
$r(C_2-C_3)$	1.505	1.512
$r(C_3-O_2)$	1.425	1.450
$r(O_2-C_4)$	1.423	1.451
$a(C_1-O_1-C_2)$	116.6	116.9
$a(O_1-C_2-C_3)$	108.3	107.6
$a(C_2-C_3-O_2)$	108.3	107.6
$a(C_3-O_2-C_4)$	116.6	116.8
$t(C_1-O_1-C_2-C_3)$	−169.4	157.9
$t(O_1-C_2-C_3-O_2)$	78.8	47.2
$t(C_2-C_3-O_2-C_4)$	−169.4	158.5
$r(C_1-H_1)$	1.078	1.077
$r(C_1-H_2)$	1.085	1.080
$r(C_1-H_3)$	1.086	1.079
$r(C_2-H_4)$	1.087	1.081
$r(C_2-H_5)$	1.084	1.081
$a(H_4-C_4-C_3)$	110.3	110.3
$a(H_5-C_4-C_3)$	109.3	111.6
$r(Li-O_1)$		1.843
$a(Li-O_1-C_2)$		107.4
$t(Li-O_1-C_2-C_3)$		−35.3
total energy	−306.8377704	−314.2034333

cies CH_2 rocking mode is 855 cm^{-1} for the TGT conformer and 894 cm^{-1} for the T0T conformer. Similarly, the frequencies of the B-type symmetry species are 868 and 858 cm^{-1}. Jaffe et al. have also calculated vibrational frequencies for the TGT conformer of this compound using D95**SCF wave functions[21] and find values of 864 and 850 cm^{-1}. The data of Murcko and DiPaola have been scaled by a factor of 0.9, which is the scale factor used by Jaffe et al. in their calculations. These calculations show that the CH_2 rocking mode belonging to the A-type species increases in frequency with decreasing O–C–C–O torsional angle between the TGT and T0T conformers, while the frequency of the B-type mode decreases with decreasing torsional angle. Based on the assumption that coordination with a lithium ion affects each ethylene oxide subunit of the diglyme in much the same manner, it is possible to make a reasonable deduction as to the nature of the local conformation in the polymer backbone induced by coordination with the cation. The relatively greater increase of the A-type mode frequency with decreasing torsional angle suggests that the new conformation stabilized by interaction with the cation has a torsional angle smaller than that which occurs in the pure liquid. We have calculated the optimized geometries and total energies of the monoglyme and its lithium complex, which are summarized in Figure 9 and Table 3. This calculation (at the HF 6-31G level) yields an O–C–C–O torsional angle of 79° for the monoglyme and 47° for the monoglyme–lithium complex.

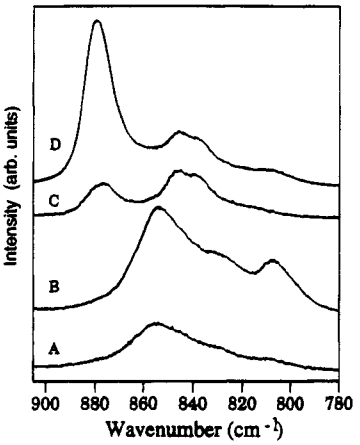

Figure 10. Polarized Raman scattering spectra of the diglyme and 5:1 diglyme–LiTf complex in the CH_2 rocking spectral region: (A) perpendicularly polarized spectrum of the pure diglyme; (B) parallel polarized spectrum of the pure diglyme; (C) perpendicularly polarized spectrum of the diglyme complex; (D) parallel polarized spectrum of the diglyme complex.

The assignment of the mode at 879 cm^{-1} in the diglyme complex to an A symmetry species is confirmed by a comparison of parallel and perpendicularly polarized Raman scattering spectra as illustrated in Figure 10, which shows the polarized spectra of both the diglyme and the diglyme–salt complex. The two modes at 846 and 836 cm^{-1} in the complex can be assigned to B-type symmetry species. These spectral data also support the approximation introduced earlier in the discussion, namely, a vibrational analysis in terms of the local symmetry of an ethylene oxide subunit. However, the polarization data for the band at 853 cm^{-1} in the pure diglyme do not allow an unambiguous assignment to either an A- or B-type symmetry species. This band is broad and may contain two modes, one of which belongs to an A-type symmetry species and the other to a B-type symmetry species. Although the calculations of Murcko and DiPaola and those of Jaffe et al. predict that the A mode is lower in frequency than the B mode in the monoglyme, the values of the frequencies are very similar. Further, the data of Murcko and DiPaola show that the rapid increase in the A mode frequency and the relatively slower decrease of the B mode frequency causes the two frequencies to cross at a torsional angle slightly smaller than that of the TGT conformation. Therefore, the polarized Raman data and the various ab initio calculations are consistent with a smaller torsional angle in the complex relative to the pure diglyme.

Another result which comes out of the ab initio calculations is the relatively small energy differences between the various conformations of the O–C–C–O moiety. Gas-phase calculations by Murcko and DiPaola and those of Jaffe et al. find that the TTT conformation is favored over the TGT conformation by values ranging from a few tenths to a few kilocalories per mole, depending on the basis set employed. The fact that the TGT conformation is experimentally observed is attributed to solution effects.[21] Since the new conformation in the glyme–salt complexes and the PEO–salt complex is achieved by a change in the O–C–C–O torsional angle which has a very low rotational energy barrier, the stabilization of this conformation by interaction with the lithium cation is not surprising.

Table 4. Infrared and Raman CH_2 Rocking Mode Frequencies (cm^{-1}) of $CH_3(OCH_2CH_2)_nOCH_3$ Complexed with Lithium Triflate (EO:M = 5:1) as a Function of Oligomer Chain Length, *n*

chain length (*n*)	Raman	infrared
monoglyme (1)	873	869
diglyme (2)	879	874
triglyme (3)	871	870
tetraglyme (4)	869	866

As noted earlier the band at 853 cm^{-1} is a mixture of CH_2 rocking motion and CO stretching motion. Although the lithium ion interacts with the ether oxygen atoms of the polymer backbone in the formation of the complex, the observed frequency shift in this band upon complexation is due to a change in the local conformation rather than a change in the electron density of the C–O bonds. Our calculations indicate a decrease in the CO stretching force constant resulting from a decrease in the electron density of these bonds. This effect by itself would be observed as a decrease in the band frequency. However, this decrease is more than offset by the frequency increase originating in the contribution from the CH_2 rocking motion to the normal mode.

It is interesting to note that the noncoincidence of the strongest Raman and infrared bands in the CH_2 rocking spectral region occurs in the diglyme–salt complex as well as the PEO–salt complex as illustrated in curves B of Figures 1 and 2. This behavior is also seen in the lithium triflate complexes of a number of glymes and is summarized in Table 4. The frequency differences range from 5 cm^{-1} in the diglyme complex to no significant difference in the triglyme complex. These observations argue that there are small differences in the local conformation induced by complexation, which depend to some extent on the chain length of the oligomer.

5. Conclusions

In an earlier study of conformation in a series of glyme–salt complexes, we speculated that a new band which was observed to increase in intensity with increasing salt concentration was due to a new conformer whose structure is stabilized through the interaction of the backbone ether oxygen atoms with the complexing cation. Although that study was limited to the Raman spectrum of the CH_2 rocking region, it is now clear that a similar pattern is observed in many different vibrational modes involving significant CH_2 motion. Polarized Raman spectra of the glyme and the glyme–salt complex in parallel and perpendicular scattering geometries establish that the intense mode in the CH_2 rocking region which shifts to higher frequency upon complexation belongs to the totally symmetric irreducible representation, i.e., an A symmetry species mode. Ab initio calculations of this frequency as a function of monoglyme conformation show that the frequency sharply increases as the O–C–C–O torsional angle decreases in passing from the TGT conformer to the T0T conformer.

The similar appearance of new bands in a number of spectral regions in both the diglyme and high molecular weight PEO upon complexation with lithium triflate suggests that similar local conformational changes are occurring in both systems. This is confirmed by comparing available structural data for the two systems. A calculation of the O–C–C–O torsional angle in the 3:1 PEO–lithium triflate compound from the X-ray diffraction data reported by Lightfoot et al. yields two torsional angles with values of 44° and 64°. The former angle is significantly smaller than the average angle of 68.4° found in crystalline PEO and is comparable with the value of 47° found from our ab initio calculation for the diglyme complex (Table 3).

Acknowledgment. This work was partially supported by funds from the National Science Foundation EPSCoR Advanced Development Program (Grant No. EHR-9108771) and the American Chemical Society (Grant No. ACS-PRF 25481-AC7P).

References and Notes

(1) Armand, M. R.; Chabagno, J. M.; Duclot, M. J. In *Fast Ion Transport in Solids*; Vashishta, P., Munday, J. N., Shenoy, G. K., Eds.; North-Holland: Amsterdam, The Netherlands, 1971; p 131.
(2) MacCallum, J. R.; Vincent, C. A. In *Polymer Electrolyte Reviews*; MacCallum, J. R., Vincent, C. A., Eds.; Elsevier: New York, 1987; Vol. 1, Chapter 2.
(3) Shriver, D. F.; Papke, B. L.; Ratner, M. A.; Dupon, R.; Wong, T.; Brodwin, M. *Solid State Ionics* **1981**, *5*, 83.
(4) Killis, A.; Le Nest, J. F.; Cheradame, H.; Gandini, A. *Makromol. Chem.* **1982**, *183*, 2835.
(5) Tadokoro, H.; Chatani, Y.; Yoshihara, T.; Tarahara, S.; Murahashi, S. *Makromol. Chem.* **1964**, *73*, 109.
(6) Chatani, Y.; Fujii, Y.; Takayanagi, T.; Homma, A. *Polymer* **1990**, *31*, 2238.
(7) Chatani, Y.; Okamura, S. *Polymer* **1987**, *28*, 1815.
(8) Iwamoto, R.; Saito, Y.; Ishihara, H.; Tadokoro, H. *J. Polym. Sci., Polym. Phys. Ed.* **1968**, *6*, 1509.
(9) Yokoyama, M.; Ishihara, H.; Iwamoto, R.; Tadokoro, H. *Macromolecules* **1969**, *2*, 184.
(10) Papke, B. L.; Ratner, M. A.; Shriver, D. F. *J. Phys. Chem. Solids* **1981**, *42*, 493.
(11) Ogawa, Y.; Ohta, M.; Sakakibara, M.; Matsuura, H.; Harada, I.; Shimanouchi, T. *Bull. Chem. Soc. Jpn.* **1977**, *50*, 650.
(12) Matsuura, H.; Fukuhara, K.; Tamaoki, H. *J. Mol. Struct.* **1987**, *156*, 293.
(13) Matsuura, H.; Fukuhara, K. *J. Polym. Sci., Part B* **1986**, *24*, 1383.
(14) Matsuura, H.; Miyazawa, T.; Machida, K. *Spectrochim. Acta* **1973**, *29A*, 771.
(15) Ohmoto, H.; Kai, Y.; Yasuoka, N.; Kasai, N.; Yanagida, S.; Okahara, M. *Bull. Chem. Soc. Jpn.* **1979**, *52*, 1209.
(16) Frech, R.; Huang, W. *Solid State Ionics* **1994**, *72*, 103.
(17) Robitaille, C. D.; Fauteux, D. *J. Electrochem. Soc.* **1986**, *133*, 315.
(18) Lightfoot, P.; Mehta, M. A.; Bruce, P. G. *Science* **1993**, *262*, 883.
(19) Takahashi, Y.; Tadokoro, H. *Macromolecules* **1973**, *6*, 672.
(20) Murcko, M. A.; DiPaola, R. A. *J. Am. Chem. Soc.* **1992**, *114*, 10010.
(21) Jaffe, R. L.; Smith, G. D.; Yoon, D. Y. *J. Phys. Chem.* **1993**, *97*, 12745.

MA941202G